Available online at www.sciencedirect.com
ScienceDirect
Ceramics International 37 (2011) 1265–1275
CERAMICS INTERNATIONAL
www.elsevier.com/locate/ceramint

Dielectric and piezoelectric properties of PZT ceramics doped with strontium and lanthanum

Volkan Kalem [a,*], İbrahim Çam [b], Muharrem Timuçin [a]

[a] Department of Metallurgical and Materials Engineering, METU, 06531 Ankara, Turkey
[b] R&D Training Center, Central Laboratory, METU, 06531 Ankara, Turkey

Received 1 June 2010; received in revised form 10 November 2010; accepted 3 December 2010
Available online 31 January 2011

Abstract

PZT based piezoelectric ceramics obtained by doping with various levels of Sr^{2+} and La^{3+}, designated as PSLZT, were prepared by conventional processing techniques. The effects of Sr^{2+} and La^{3+} additions, and that of the Zr/Ti ratio on microstructure, on phase constitution, and on the dielectric and piezoelectric properties were investigated. XRD data revealed that all PSLZT compositions had perovskite structure in which increasing Sr and/or decreasing Zr/Ti ratio increased the tetragonality. In PSLZT ceramics the morphotropic phase boundary (MPB) appeared as regions extending from Zr/Ti ratio of 52/48 to 58/42. Among all compositions studied, the PSLZT ceramic having 5 at% Sr^{2+} and 1 at% La^{3+} with a Zr/Ti ratio of 54/46 exhibited a peak piezoelectric strain coefficient of d_{33} = 640 pC/N with attending dielectric and electromechanical parameters K_{33}^{T} = 1800, k_p = 0.56, Q_m = 70, and tan δ = 1.55%.

Keywords: C. Dielectric properties; C. Piezoelectric properties; D. PSLZT

1. Introduction

Piezoelectric ceramics based on lead–zirconate–titanate (PZT) are widely used for numerous applications in the microelectronics industry. In order to tailor the physical properties required in specific applications, PZT ceramics are usually doped with small amounts of other oxides. The compositions neighboring the morphotropic phase boundary (MPB) exhibit enhanced piezoelectric activity; therefore the Zr/Ti ratio in the ceramic has also been given an important consideration in the production of PZT ceramics. The effects of Zr/Ti ratio and those of different additives on the structural and electrical properties of PZT ceramics were investigated extensively in various earlier studies [1–8].

Present study is concerned with the PSLZT ceramics which have dual incorporation of Sr and La into the PZT. Sr is an isovalent additive substituting for Pb on the A site in the perovskite structure. It has entered into the formulation of a large number of PZT ceramics, including both the soft and the hard types. Sr additions exhibited improved dielectric permittivity, ε, and larger piezoelectric strain coefficient, d_{31}, with slight increase in the electromechanical coupling factor, k_p, These effects were attributed to the straining of the PZT lattice due to the smaller size of Sr as compared to that of the parent Pb [9–12]. The ceramic with composition $Pb_{0.95}Sr_{0.05}Zr_{0.53}Ti_{0.47}O_3$ or $Pb_{0.94}Sr_{0.06}Zr_{0.53}Ti_{0.47}O_3$ has been denoted as the basis for the commercial PZT4 [13,14]. Such ceramics were shown to exhibit favorable depoling characteristics [15].

Because the size of the La^{3+} ion (0.136 nm) is compatible with that of Pb^{2+} (0.149 nm) it has been used as an additive to PZT in manufacturing two different types of PLZT ceramics. The compositions rich in ZrO_2 have been hot pressed for use in electrooptic applications due to their transparency and high photostriction. The notable composition developed for this purpose was a ZrO_2-rich hot-pressed PLZT denoted as 9/65/35, the ratio standing for the atomic percentages of La/Zr/Ti [16]. The second group of PLZT ceramics has much lower ZrO_2 content; their compositions lie closer to or within the MPB region. Large improvements were obtained in dielectric permittivity and piezoelectric strain coefficient when small additions (usually <2 wt%) of La_2O_3 was made as a donor

* Corresponding author. Tel.: +90 312 210 5913; fax: +90 312 210 2518.
E-mail address: vkalem@metu.edu.tr (V. Kalem).

0272-8842/$36.00
doi:10.1016/j.ceramint.2010.12.003

dopant to various PZT compositions [17–22]. The highest piezoelectric strain coefficient reported in the literature for a MPB type pure PLZT ceramic was achieved in the composition $Pb_{0.97}La_{0.03}(Zr_{0.53}Ti_{0.47})O_3$; the value attained was d_{33} = 455 pC/N [23].

Although the literature on the dielectric and piezoelectric properties of PSZT and PLZT type ceramics is wealthy, similar information on the PSLZT ceramics is rather scarce. Kulcsar [24] showed that dielectric permittivity and the radial piezoelectric strain coefficient could be enhanced upon incremental additions of La_2O_3 into the base $Pb_{0.95}Sr_{0.05}(Zr_{0.54}Ti_{0.46})O_3$ ceramic. However, his results were rather inconsistent and the synergy emanating from dual doping of Sr and La was not clear. Mehta et al. [25] examined the structural changes in $Pb_{0.94}Sr_xLa_y(Zr_{0.52}Ti_{0.48})O_3$ in terms of the variation in the tetragonality index as a function of co-doping. They provided no data on electromechanical properties. Recent data obtained by Ramam and Chandramouli [26] on the effects of Sr substitution into a PZT which contained La and Mn as co-dopants was limited to a ceramic of fixed composition. The effects of variations in the parameters like Zr/Ti ratio and La content were not examined and the amount of Sr addition was confined to ≤1 at%. In view of the scarcity of information on electromechanical properties of PSLZT ceramics the focus of the present study was to examine in detail the effects of (Sr, La) co-doping on the dielectric and piezoelectric properties of PZT ceramics and the changes in the associated microstructures.

2. Experimental

2.1. Ceramic preparation

High purity powders of PbO, $SrCO_3$, La_2O_3, TiO_2 (Merck) and ZrO_2 (SEPR-CS10) were used to prepare the desired compositions of PSLZT ceramics by the mixed-oxide method. The oxide constituents were weighed in accordance with the molecular formula $Pb_{1-x-y}Sr_xLa_y(Zr_zTi_{1-z})_{1-(y/4)}O_3$ (x = 0.0–0.05, y = 0.0–0.05, and z = 0.5–0.6). This formulation was preferred due to the enhanced sinterability stemming from the slight excess (∼0.5 wt%) of PbO over the A-site formula despite the fact that the charge neutrality condition is met by forming vacancies on both the A and B sites of the perovskite lattice [17,18]. Each powder batch was blended thoroughly in an agate mortar and pestle under ethanol. The dried mixture was compacted as a slug in a hardened steel die and then calcined at 820 °C for 2 h. The product was ball milled for 12 h; it was dried and then given a second calcination at 850 °C for 2 h. The final slug was crushed and ball milled in a plastic vial for 16 h. All millings were done with stabilized zirconia balls in a medium of ethanol. The average particle size of the powder obtained by this process, determined with a Malvern Mastersizer 2000 laser particle size analyzer, was about 1 μm.

Green ceramic discs, each measuring 13 mm in diameter and 1 mm in thickness, were prepared from the PSLZT powders plasticized by 3 wt% PEG addition. The discs were compacted by uniaxial pressing in a hardened tool steel die under a load of 150 MPa. After binder burnout in air at 600 °C, the discs were sintered by soaking at 1240 °C for 2 h in a closed saggar assembly which contained PSLZT bedding to inhibit PbO evaporation from the ceramic samples. In line with the suggestions made by Mohiddon and Yadav [27], the rates during heating to the soaking temperature and cooling afterwards were kept at 4 °C/min.

2.2. Characterization

The densities of sintered ceramics were determined by the liquid displacement technique based on the Archimedes' principle. Xylene was the immersion fluid. The microstructural studies were conducted mainly on polished sections under a FEI Nova Nano 430 FEG scanning electron microscope (SEM). The polished surfaces were given a thermal etch at 1000 °C for 1 h in enclosures containing PZT bedding to compensate for PbO loss. Preceding the SEM work, the sample surfaces were sputtered with gold. The average grain size was calculated on the SEM micrographs by the usual linear intercept method [28]. The extent of porosity in the ceramics was also ascertained from examination of their fracture surfaces under SEM.

XRD analyses were performed for monitoring the powder synthesis process, for determination of the lattice parameters, and quantification of the tetragonal, T, and rhombohedral, R, phase fractions present in sintered ceramics. A Rigaku D/max2200/PC model diffractometer was used with Cu-Kα radiation, the diffraction data were collected over the 2θ range from 20 to 70° with a step size of 0.02°.

For electromechanical measurements, the flat surfaces of the sintered discs were lapped and then metalized with a silver paste. Painted silver electrodes were fired at 750 °C for 20 min. For the poling process, the electroded discs were exposed to a DC electric field of 3 kV/mm for 30 min in a silicon oil bath at 120 °C.

The piezoelectric strain coefficient (d_{33}) of each disc was measured 24 h after poling, by a Berlincourt D33-meter. k_p and Q_m were determined by the resonance/anti-resonance method according to the IRE standards using a HP4194A impedance analyzer. The parameters k_p and Q_m were related to the resonance frequencies by means of the following expressions [29,30]:

$$k_p = \left[\frac{f_a - f_r}{0.395 f_r + 0.574(f_a - f_r)}\right]^{1/2} \quad (1)$$

$$Q_m = \frac{f_a^2}{2\pi Z_m C f_r (f_a^2 - f_r^2)} \quad (2)$$

where f_r is the resonant frequency and f_a is the antiresonant frequency in the fundamental vibration mode. Z_m and C represent the resonant impedance and the capacitance on the mechanical branch of the equivalent circuit, respectively. The reliability of the data was checked by conducting measurements on duplicate samples, the experimental uncertainty was confined to ±4% of the reported values.

The dielectric properties, free dielectric constant (K_{33}^T) and loss tangent (tan δ), of the poled ceramics were calculated from

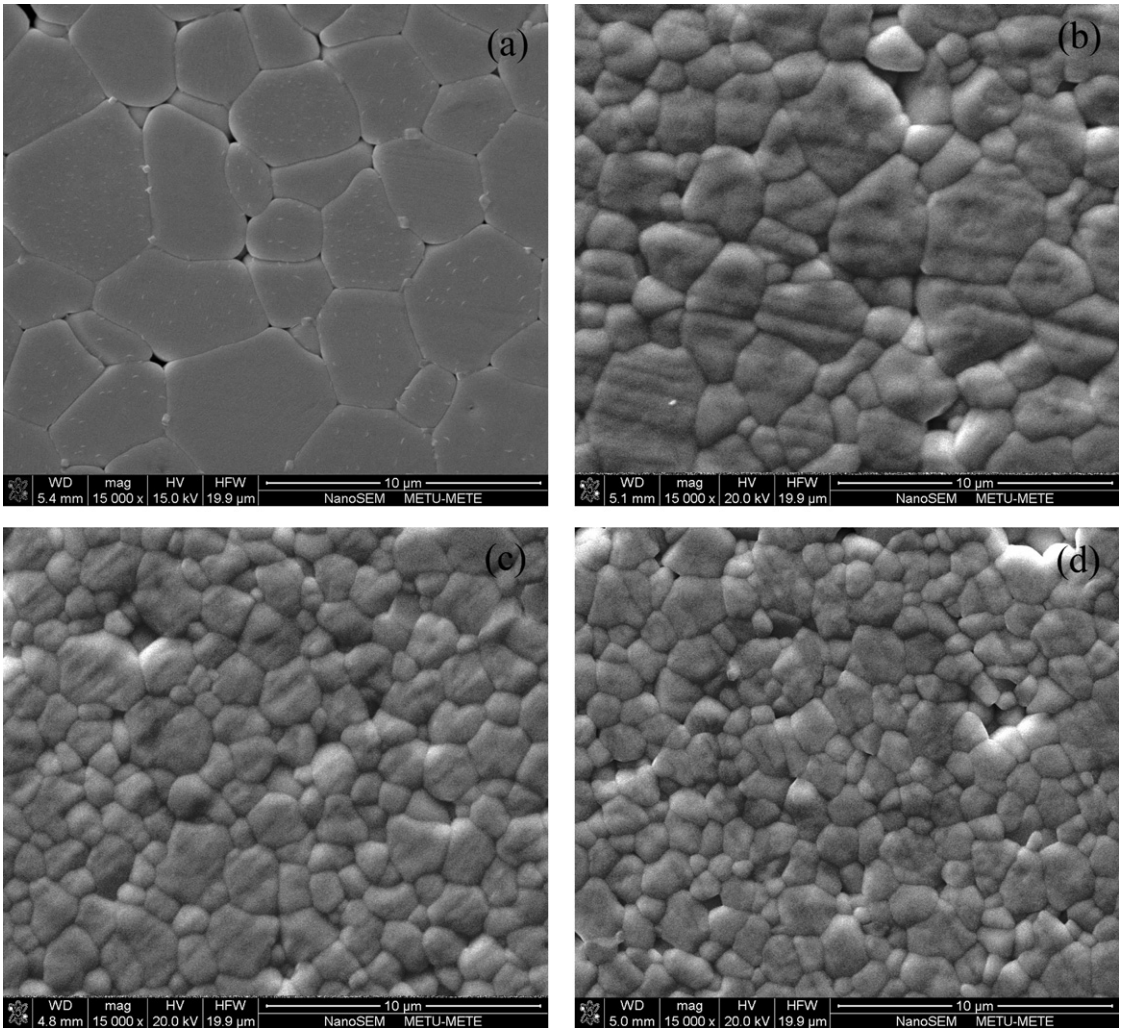

Fig. 1. SEM micrographs of $Pb_{0.95-y}Sr_{0.05}La_y(Zr_{0.54}Ti_{0.46})O_3$ ceramics with increasing La content: (a) $y = 0.00$, (b) $y = 0.01$, (c) $y = 0.04$, and (d) $y = 0.05$.

the capacitance and dissipation factor values measured at 1 kHz and sample dimensions. Hysteresis behavior was characterized with a modified Sawyer-Tower circuit at 25 °C using a 50 Hz driving field. The Curie temperature, T_C, of poled discs was determined by establishing the variation of dielectric permittivity with temperature in the range 100–350 °C. These measurements were done at 1 kHz frequency by placing the samples in a small pot furnace in which the data on permittivity were taken upon cooling the ceramics from high temperature at a rate of 3 °C/min.

3. Results and discussion

3.1. $Pb_{0.95-y}Sr_{0.05}La_y(Zr_{0.54}Ti_{0.46})O_3$ ceramics

The PSZT ceramic selected for modification by La was the PZT having 5 at% Sr and a Zr/Ti ratio of 54/46. The selection was based on a preliminary compositional screening with respect to an optimized combination of electromechanical properties attainable within the MPB region of $Pb_{0.95}Sr_{0.05}Zr_{1-z}Ti_zO_3$ ceramics. The $d_{33} = 305$ pC/N measured for the ceramic $Pb_{0.95}Sr_{0.05}Zr_{0.54}Ti_{0.46}O_3$ matched perfectly with the one reported by Lal et al. [12] for their MPB composition. It should be noted that the MPB region of the PSZT ceramics studied in the present work was broader than the one reported by Lal et al. [12] due to differences in methods of ceramic powder synthesis.

The ceramic $Pb_{0.95}Sr_{0.05}Zr_{0.54}Ti_{0.46}O_3$ was modified by partial substitution of La^{3+} ions for Pb^{2+} with increasing levels of La up to 5 at% replacement in the molecular formula of the PSLZT. The data on various physical properties of these ceramics are given in Table 1.

The densification behavior was rather complex; at lower levels of La the ceramics attained higher densities than the base PSZT, but the densification became poorer above 4 at% La due probably to reduced rates of volume diffusion reflected in smaller grain size. The SEM micrographs shown in Fig. 1 revealed that average grain size decreased continuously with increased La substitution. The reduction in the grain size has been attributed to the solid solution impurity drag mechanism in which the La ion concentration gradient present at grain boundaries was claimed to cause blocking of grain boundary mobility leading to substantially slower grain growth rate [29].

Table 1
Physical properties of $Pb_{0.95-y}Sr_{0.05}La_y(Zr_{0.54}Ti_{0.46})O_3$ ceramics.

y	0.000	0.005	0.010	0.020	0.030	0.040	0.050
d_{33} (pC/N)	305	490	640	535	490	430	425
k_p	0.44	0.51	0.56	0.52	0.50	0.46	0.42
Q_m	345	92	70	78	76	76	71
K_{33}^T	1138	1347	1800	1963	1944	1850	1460
tan δ (%)	0.44	1.40	1.55	1.55	1.65	1.77	1.86
Density as %TD	96.94	97.80	98.29	98.78	98.78	97.38	96.63
Average grain size, μm	4.51	4.02	3.62	2.93	2.52	2.21	1.75

The XRD patterns of the $Pb_{0.95-y}Sr_{0.05}La_y(Zr_{0.54}Ti_{0.46})O_3$ ceramics are shown in Fig. 2. At all levels of La addition, the perovskite PSLZT consisted of a mixture of T and R phases. The overlapping triplet peaks from the (2 0 0)T, (2 0 0)R, and (0 0 2)T planes in the 2θ range 43–46° were deconvoluted using the Lorenzian profile function [21], and the relative volume fractions of rhombohedral and tetragonal phases, %R and %T, were estimated from the intensities $I_{(2\,0\,0)R}$, $I_{(2\,0\,0)T}$, and $I_{(0\,0\,2)T}$ through the following relationships:

$$\%R = \frac{I_{(200)R}}{I_{(200)T} + I_{(200)R} + I_{(002)T}}, \quad \%T = 100 - \%R \qquad (3)$$

The calculations on the relative proportions of the T and R phases in this group of PSLZT ceramics as a function of La content led to the distribution shown in Fig. 3. Obviously, La additions did not destroy the stability of the T phase. This observation is somehow different than the findings of Hammer and Hoffmann [21]. According to their XRD work on the PLZT solid solutions with Zr/Ti ratio of 53/47, the T phase content showed fluctuations with varying levels of La addition. The greater stability obtained in the relative amount of the T phase in this work may be linked with the coexistence of Sr and La.

The variations in the piezoelectric properties of $Pb_{0.95-y}Sr_{0.05}La_y(Zr_{0.54}Ti_{0.46})O_3$ ceramics with La content are shown in Fig. 4. A small amount of La substitution in the base PSZT caused a large jump in the piezoelectric strain coefficient d_{33} which exhibited a peak value of 640 pC/N at 1 at% La. Additions of La beyond this limit resulted in reduced d_{33} values. The same trend was observed in k_p and K_{33}^T. The curve for K_{33}^T exhibited a rather diffuse pattern which may be attributed to the gradual reduction of coupling, caused by increased La substitution, between $(Zr,Ti)O_6$ octahedra and the A site occupants [30].

The complex behavior observed for d_{33}, k_p, and K_{33}^T in Fig. 4 was attributed to the competition between the vacancy effect and the grain growth inhibition brought by La, both being manifested in the movement of domain walls. In the PSLZT ceramics of interest, the T phase was dominant which means that the 180° domains and 90° domains belonging to this modification are of importance. During the poling process, virtually all 180° domains are oriented along the poling direction; therefore the 90° domains gain further significance. At low levels of La, the vacancies introduced by doping facilitate the rotation of 90° domains and promote the motion of the 90° domain walls leading to enhancement in electromechanical properties. On the other hand, additions of La cause reduction in the grain size which implies that the domain size is also reduced [31]. Furthermore, the porosity increase at La levels above 3 at%. Under these conditions, the domains get clamped gradually by increasing La substitution due to the pinning action of grain boundaries and the dominance of space charge effects [32]. Hence, reductions in the electromechanical properties are observed at higher levels of La doping. The

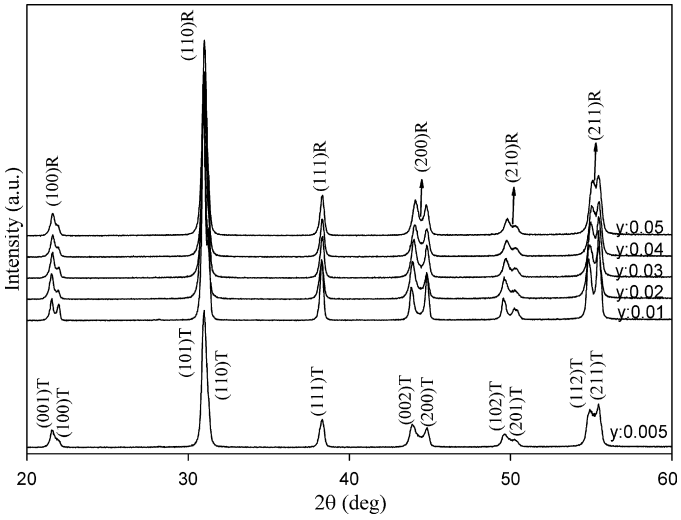

Fig. 2. The XRD patterns of the $Pb_{0.95-y}Sr_{0.05}La_y(Zr_{0.54}Ti_{0.46})O_3$ ceramics.

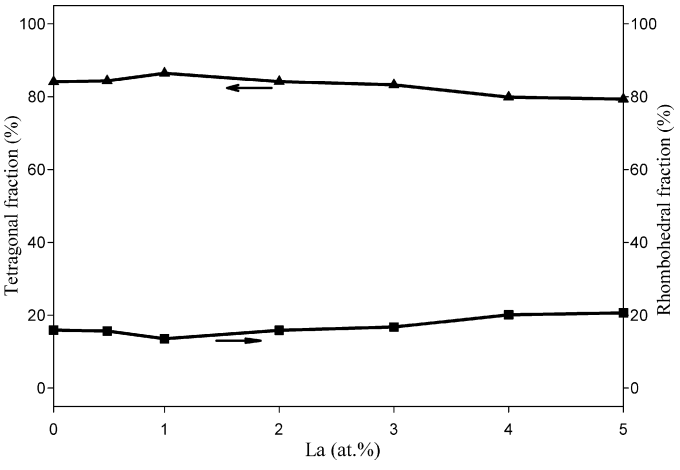

Fig. 3. The proportions of phases T and R in the $Pb_{0.95-y}Sr_{0.05}La_y(Zr_{0.54}Ti_{0.46})O_3$ ceramics as a function of La doping.

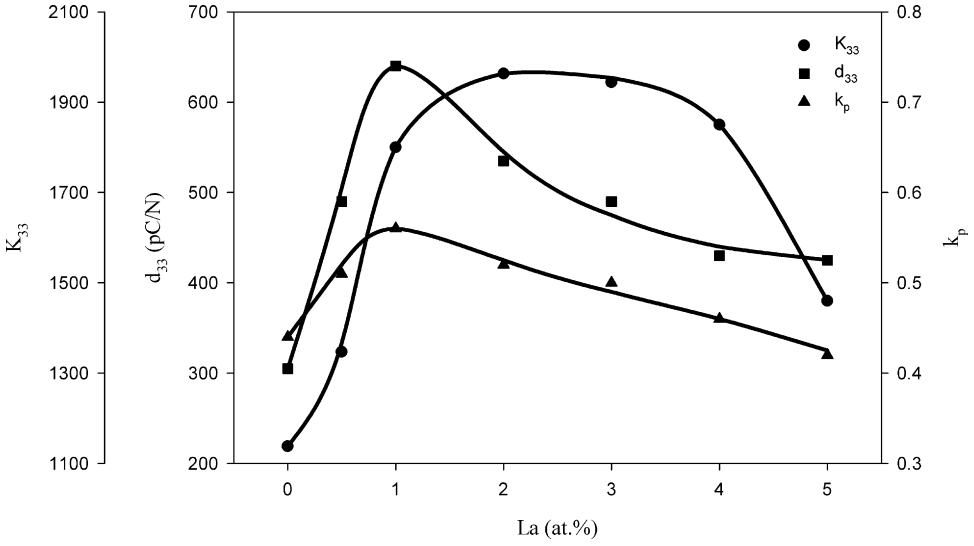

Fig. 4. Variations in the dielectric and piezoelectric properties of $Pb_{0.95-y}Sr_{0.05}La_y(Zr_{0.54}Ti_{0.46})O_3$ ceramics with increasing La substitution.

addition of La made the PSZT ceramic a soft piezoelectric as can be seen in Fig. 5. The material assumed lossy characteristics upon the smallest La substitution.

3.2. $Pb_{0.94}Sr_{0.05}La_{0.01}(Zr_{1-z}Ti_z)O_3$ ceramics

The data on physical properties of PSLZT ceramics with 1 at% La, 5 at% Sr and variable Zr/Ti content are given in Table 2. Based on comparison with x-ray densities, the ceramics densified to better than 97% of the theoretical. SEM observations on fracture surfaces also revealed limited porosity. The average grain size was not affected much by the Zr/Ti ratio. The effective packing of the grains, seen in the SEM micrographs of the thermally etched surfaces in Fig. 6 may be the reason for good densification.

Fig. 7 shows XRD patterns of the $Pb_{0.94}Sr_{0.05}La_{0.01}(Zr_z-Ti_{1-z})O_3$ ceramics. The patterns revealed the co-existence of T and R modifications. The proportions of T and R phases in the MPB are displayed in Fig. 8. The MPB region was located within the range of Zr/Ti extending from 52/48 to 58/42. Inside this region, the change in the lattice constants and tetragonality with the Zr/Ti ratio is shown in Fig. 9. The tetragonality index of 1.021 and the a_R value of 4.067 Å at the Zr/Ti ratio of 52/48 were consistent with the values determined by Mehta et al. [25] for the $Pb_{0.94}Sr_xLa_y(Zr_{0.52}Ti_{0.48})O_3$ ceramics with La/Sr ratio similar to the present work.

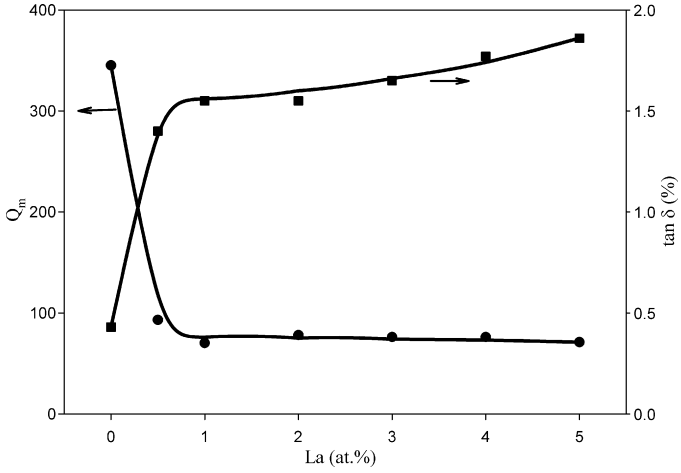

Fig. 5. Variations in Q_m and tan δ with La content in $Pb_{0.95-y}Sr_{0.05}La_y(Zr_{0.54}Ti_{0.46})O_3$ ceramics.

In contrast to the situation observed on grain size, the piezoelectric and dielectric properties were highly sensitive to the Zr/Ti ratio. The dielectric and piezoelectric properties of the $Pb_{0.94}Sr_{0.05}La_{0.01}(Zr_zTi_{1-z})O_3$ group ceramics, displayed in Fig. 10, exhibited changes typical of MPB compositions. The piezoelectric strain coefficient d_{33}, the electromechanical coupling coefficient k_p, and the dielectric constant K_{33}^T exhibited visible maxima at Zr/Ti ratio of 54/46. The maxima in these parameters were due to the coexistence of the

Table 2
Physical properties of $Pb_{0.94}Sr_{0.05}La_{0.01}(Zr_zTi_{1-z})O_3$ ceramics.

z	0.50	0.52	0.54	0.56	0.58	0.60
d_{33} (pC/N)	393	480	640	560	427	380
k_p	0.39	0.42	0.56	0.53	0.42	0.40
Q_m	96	83	70	84	99	115
K_{33}^T	972	1475	1800	1138	608	487
tan δ (%)	1.15	1.46	1.55	1.89	2.22	2.34
Density as %TD	98.12	97.98	98.29	98.36	97.23	97.48
Average grain size, μm	3.31	3.44	3.62	3.64	3.64	3.70

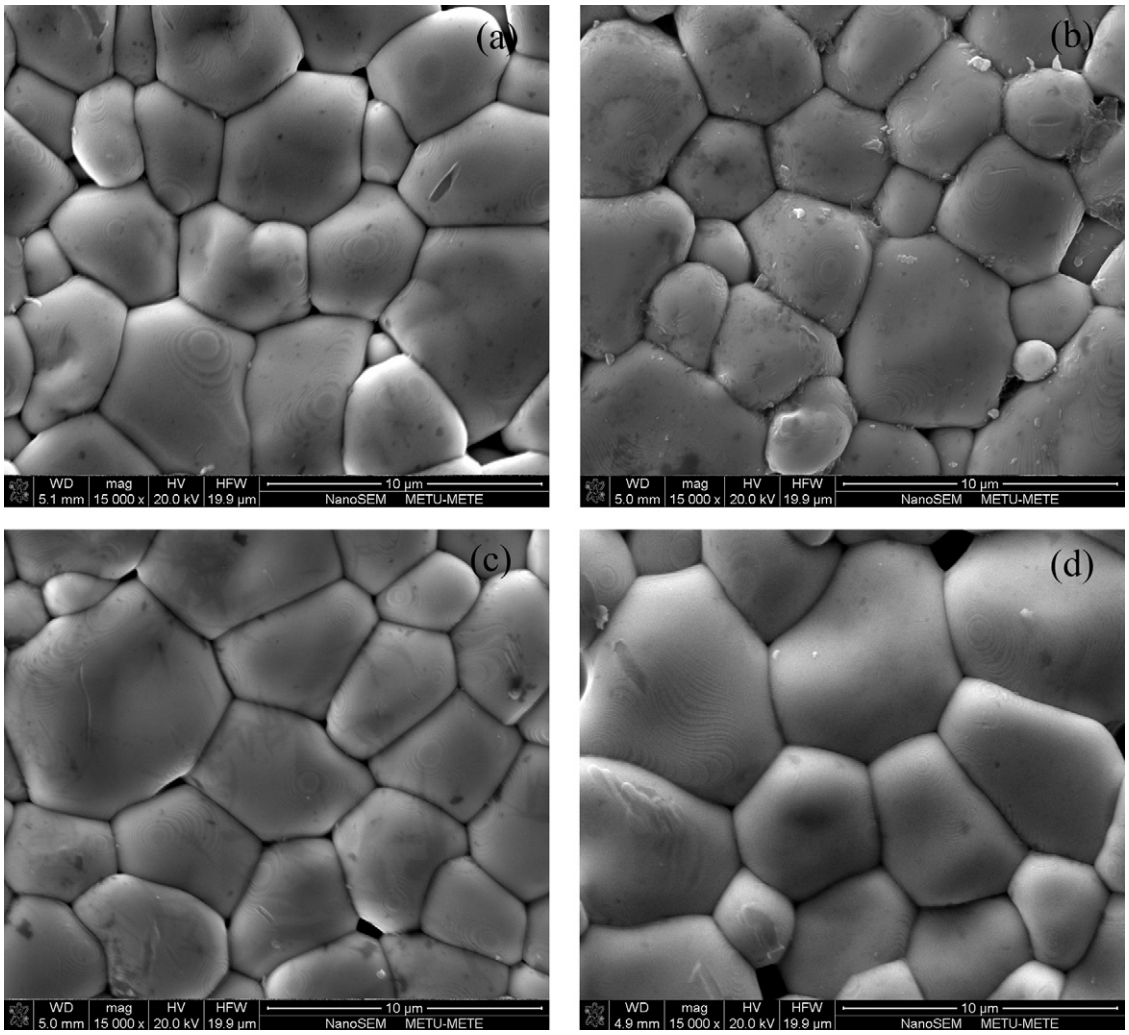

Fig. 6. SEM micrographs of the thermally etched surfaces of the $Pb_{0.94}Sr_{0.05}La_{0.01}(Zr_zTi_{1-z})O_3$ ceramics with Zr content of (a) $z = 0.52$, (b) $z = 0.54$, (c) $z = 0.58$, (d) $z = 0.60$.

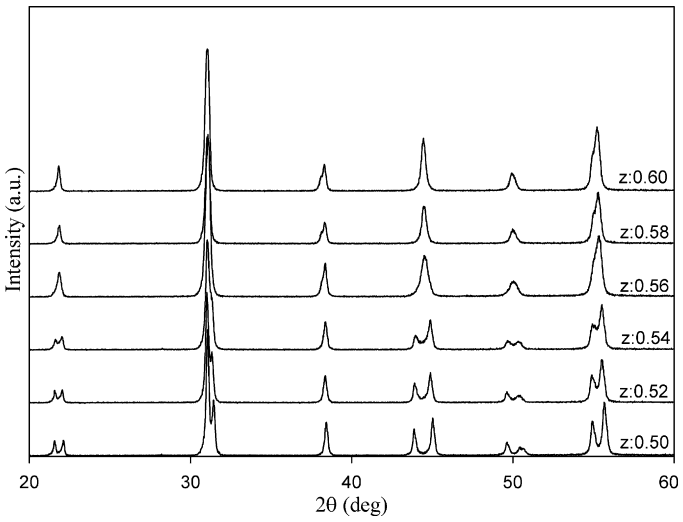

Fig. 7. The XRD patterns of the $Pb_{0.94}Sr_{0.05}La_{0.01}(Zr_zTi_{1-z})O_3$ ceramics.

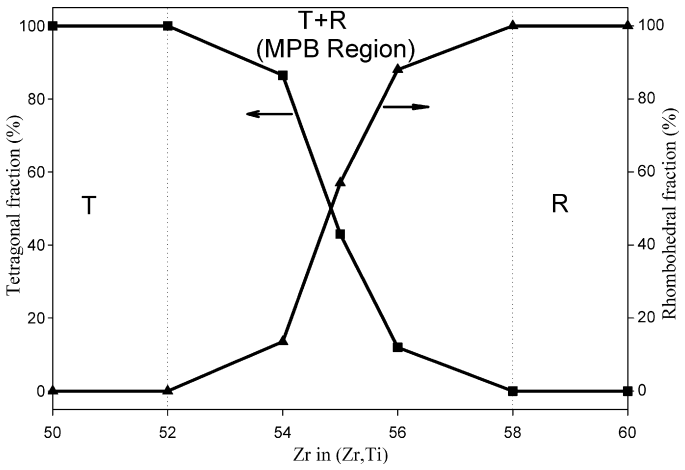

Fig. 8. Relative proportions of tetragonal and rhombohedral modifications in $Pb_{0.94}Sr_{0.05}La_{0.01}(Zr_zTi_{1-z})O_3$ ceramics.

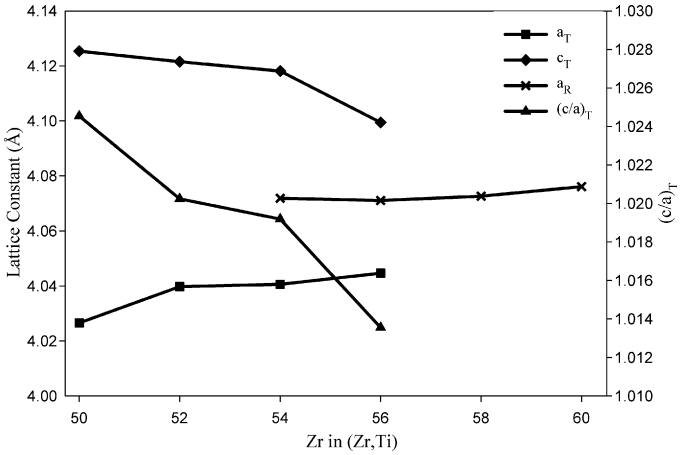

Fig. 9. The variations in lattice parameters of the T and R phases in the $Pb_{0.94}Sr_{0.05}La_{0.01}(Zr_zTi_{1-z})O_3$ ceramics.

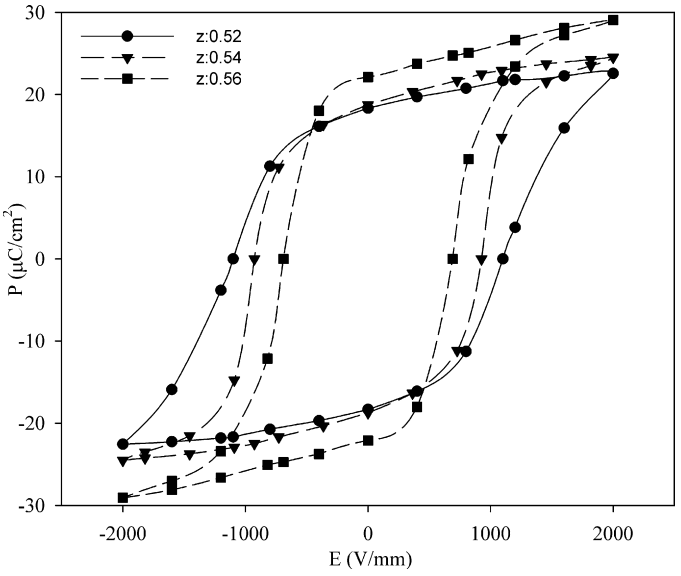

Fig. 11. The hysteresis behavior in $Pb_{0.94}Sr_{0.05}La_{0.01}(Zr_zTi_{1-z})O_3$ ceramics.

tetragonal (T) and the rhombohedral (R) phases which lead to high levels of electromechanical response. The enhanced piezoelectric activity within the transition MPB region has been attributed to the presence of a large number of energetically equivalent states allowing a high degree of alignment of ferroelectric dipoles and improved polarizability of the ceramic [1].

Hysteresis behavior of the $Pb_{0.94}Sr_{0.05}La_{0.01}(Zr_zTi_{1-z})O_3$ ceramics are displayed by the polarization curves shown in Fig. 11. These PSLZT ceramics could be polarized rather easily. In all samples the coercive field, E_c, was equal to or smaller than 1 kV/mm, comparable to the magnitude of the E_c reported earlier for PLZT ceramics [31]. The ceramics with lower Zr/Ti ratio exhibited loops of ferroelectrically harder PZT ceramics owing to the dominance of the T phase. The increase in the Zr/Ti ratio resulted in higher remanance and lower coercive field, as shown in Fig. 12. The area occupied by the hysteresis loop, which is a measure of polarization energy, became increasingly smaller as the Zr content was raised. These features are correlated well with the increased proportion of the rhombohedral phase in PZT compositions having relatively higher Zr level [33].

3.3. $Pb_{0.99-x}Sr_xLa_{0.01}(Zr_{0.54}Ti_{0.46})O_3$ ceramics

The effect of Sr content on the dielectric and piezoelectric properties of $Pb_{0.99-x}Sr_xLa_{0.01}(Zr_{0.54}Ti_{0.46})O_3$ ceramics was studied by changing the Sr-content from 0 to 5 at%. Various physical properties measured in this system are listed in Table 3. The densification was improved with increasing Sr substitution in PLZT. Sr was instrumental in grain growth as evidenced by the SEM micrographs shown in Fig. 13. The average grain size in the PSLZT ceramic doped with 5 at% Sr rose to 3.62 μm as opposed to 1.4 μm in the PLZT having no Sr.

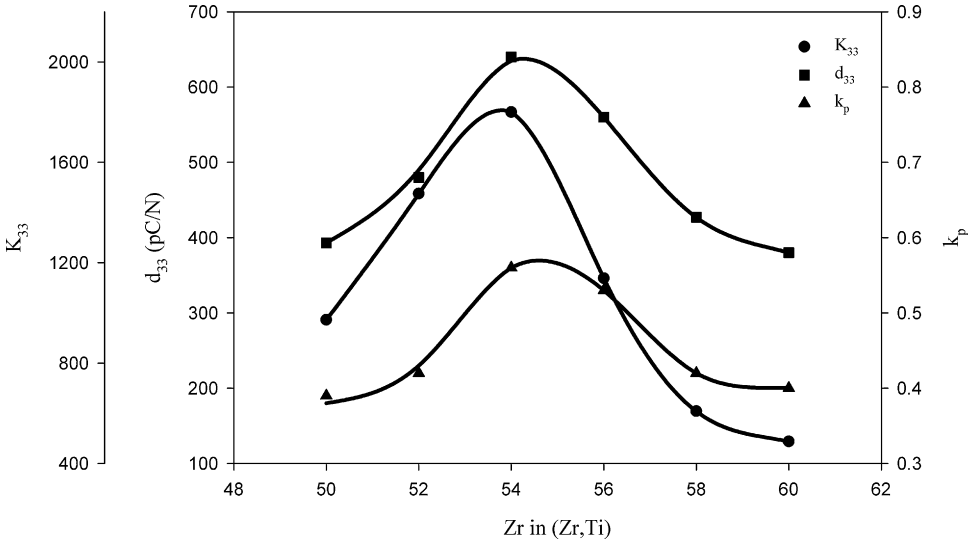

Fig. 10. Variations in the dielectric and piezoelectric properties of $Pb_{0.94}Sr_{0.05}La_{0.01}(Zr_zTi_{1-z})O_3$ ceramics.

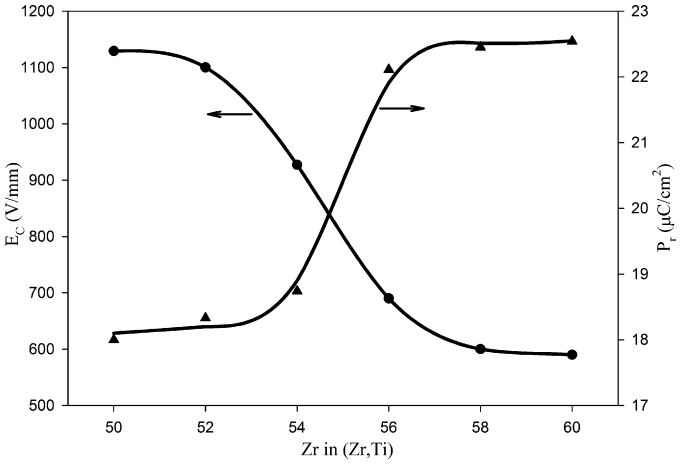

Fig. 12. Variation of coercive field and remnant polarization with Zr/Ti ratio in $Pb_{0.94}Sr_{0.05}La_{0.01}(Zr_zTi_{1-z})O_3$ ceramics.

The XRD patterns shown in Fig. 14, and the fractions of T and R phases given in Fig. 15 revealed that the tetragonal phase formation was favored at all levels of Sr substitution. The proportion of the T phase increased steadily from 55 vol% in the Sr-free PLZT ceramic to 83 vol% as Sr was raised to 5 at%.

Fig. 16 shows the changes in the dielectric and piezoelectric properties of the $Pb_{0.99-x}Sr_xLa_{0.01}(Zr_{0.54}Ti_{0.46})O_3$ ceramics. With increasing Sr substitution the dielectric constant K_{33}^T exhibited a continuous rise, indicating a steady enhancement in polarization due to the elimination of the effect of compression of the 180° domains in the T phase [34]. The effect of Sr on the piezoelectric strain coefficient was more striking; the parameter d_{33} was a modest 260 pC/N in the PLZT without Sr but it raised to 610 pC/N with 3 at% substitution of Sr for Pb. Seemingly, the piezoelectric activity reached near saturation at 3 at% Sr addition. Planar coupling coefficient showed steady improvement with Sr, but the loss tangent was not affected drastically from the presence of Sr in PLZT.

The deflection in the d_{33} curve at 3 at% Sr substitution is reflected in the dynamic polarization behavior of the PSZLT ceramics as depicted by the hysteresis curves shown in Fig. 17. The hysteresis loops could be classified under two major groups. The loops of the ceramics with low Sr were round in shape; these had smaller grain size and they exhibited lower

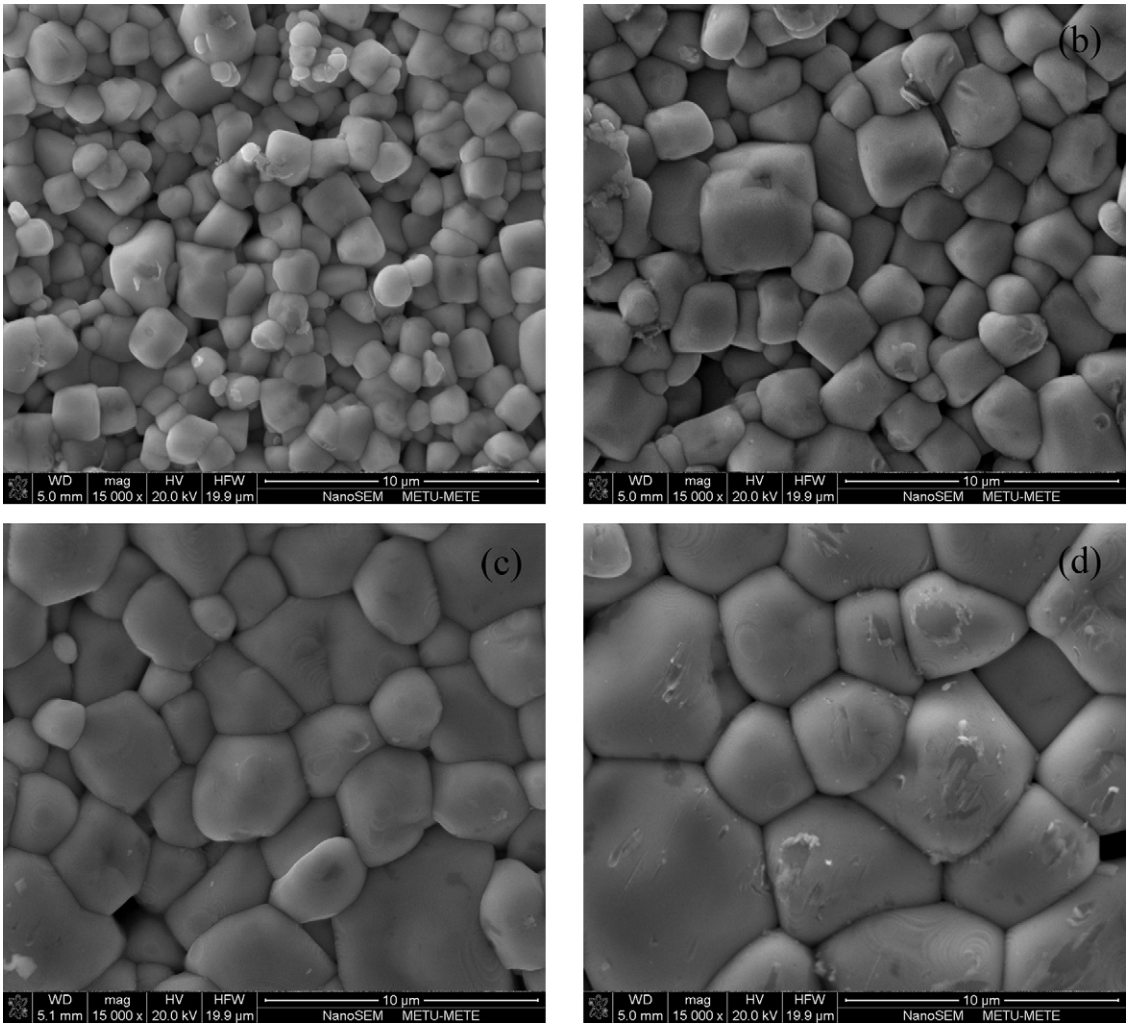

Fig. 13. SEM micrographs of the $Pb_{0.99-x}Sr_xLa_{0.01}(Zr_{0.54}Ti_{0.46})O_3$ ceramics modified with various levels of Sr addition: (a) undoped, (b) $x = 0.02$, (c) $x = 0.04$, and (d) $x = 0.05$.

Table 3
Physical properties of $Pb_{0.99-x}Sr_xLa_{0.01}(Zr_{0.54}Ti_{0.46})O_3$ ceramics.

x	0.00	0.01	0.02	0.03	0.04	0.05
d_{33} (pC/N)	260	400	505	610	625	640
k_p	0.40	0.48	0.49	0.52	0.54	0.56
Q_m	55	58	63	60	67	70
K_{33}^T	810	895	1020	1240	1520	1800
tan δ (%)	1.60	1.64	1.48	1.50	1.55	1.55
Density as %TD	94.06	95.62	96.25	96.89	97.83	98.29
Average grain size, μm	1.40	1.60	2.00	2.75	3.25	3.62

electromechanical coupling. The ceramics having Sr ≥ 3 at% had square-like hysteresis loops; they had higher k_p, and their remanance was also higher due to the increased freedom of domains emanating from removal of the clamping effect on domains which is associated with larger grain size.

The coercive field and remanance values in the low Sr group can be compared with the data provided by Nasar et al. [35] on the $Pb(Zr_{0.53}Ti_{0.47})O_3$ ceramics doped with up to 1.5 at% Sr. Their results for the ceramic with 1.5 at% Sr were E_c = 780 V/mm, and P_r =8.9 μC/cm^2. The values determined for the low-Sr group ceramics of this study, shown in Fig. 18, were quite comparable; E_c = 720 V/mm, and P_r = 8.5 μC/cm^2.

Temperature dependence of the dielectric constant of the $Pb_{0.99-x}Sr_xLa_{0.01}(Zr_{0.54}Ti_{0.46})O_3$ ceramics is displayed by the curves in Fig. 19. There was a continuous decrease in the Curie temperature (T_C) with increasing Sr addition. The Curie

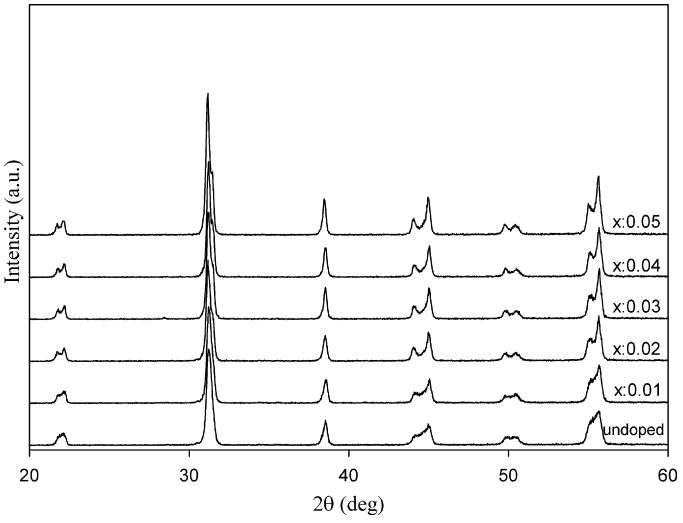

Fig. 14. The XRD patterns of the $Pb_{0.99-x}Sr_xLa_{0.01}(Zr_{0.54}Ti_{0.46})O_3$ ceramics.

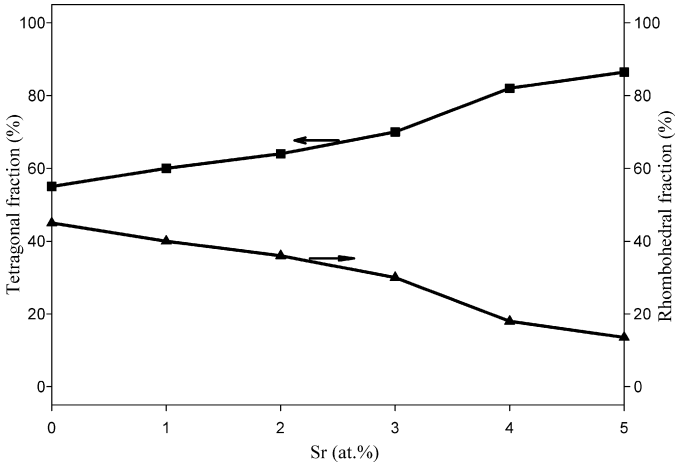

Fig. 15. T and R proportions in $Pb_{0.99-x}Sr_xLa_{0.01}(Zr_{0.54}Ti_{0.46})O_3$ ceramics with variable Sr content.

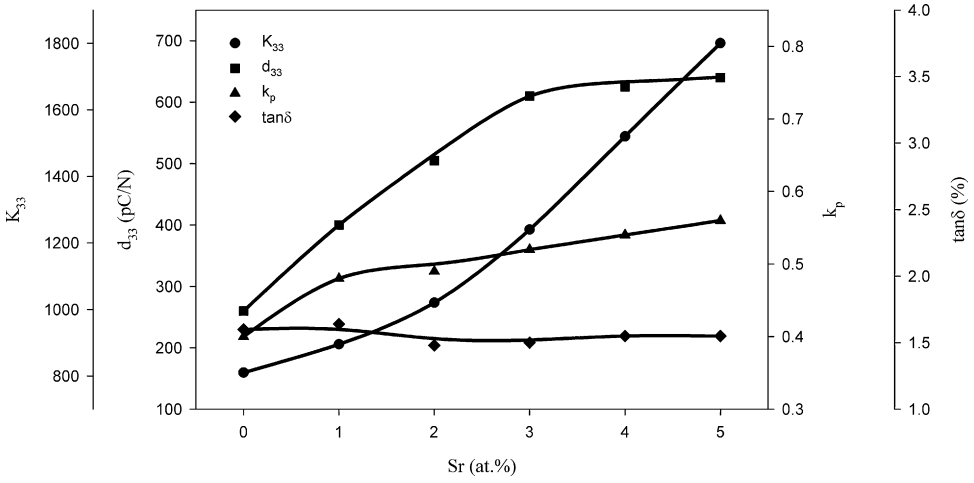

Fig. 16. Variations in the dielectric and piezoelectric properties of $Pb_{0.99-x}Sr_xLa_{0.01}(Zr_{0.54}Ti_{0.46})O_3$ ceramics.

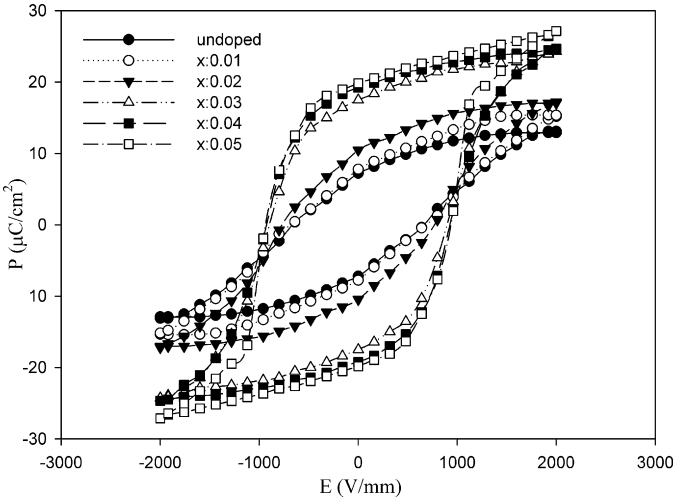

Fig. 17. Ferroelectric hysteresis loops of $Pb_{0.99-x}Sr_xLa_{0.01}(Zr_{0.54}Ti_{0.46})O_3$ ceramics.

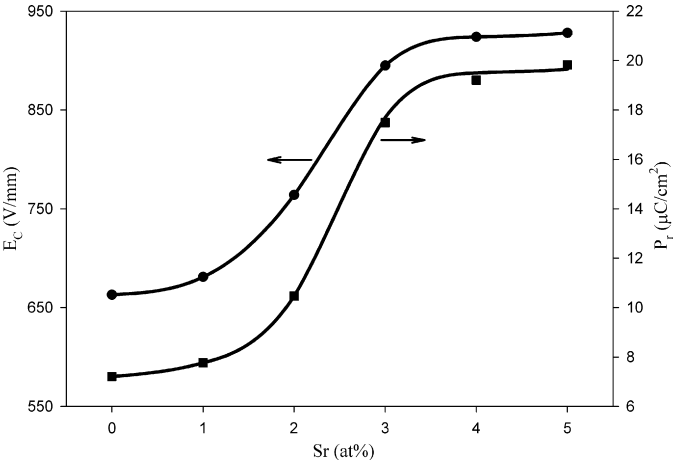

Fig. 18. Variation of coercive field and remnant polarization with Zr/Ti ratio in $Pb_{0.99-x}Sr_xLa_{0.01}(Zr_{0.54}Ti_{0.46})O_3$ ceramics.

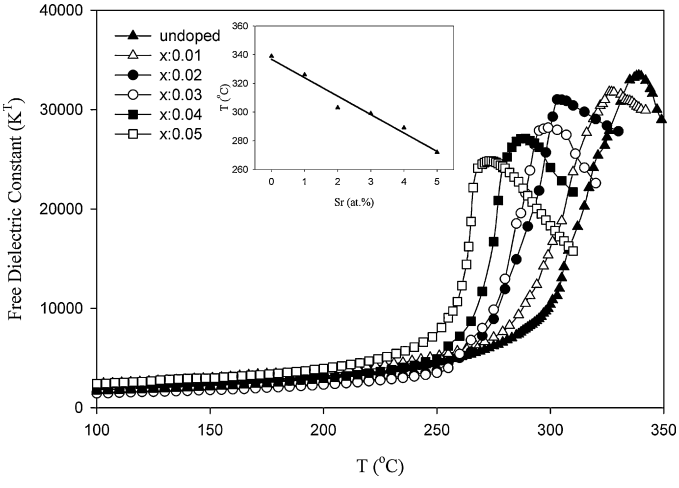

Fig. 19. The change in the dielectric constant of the $Pb_{0.99-x}Sr_xLa_{0.01}(Zr_{0.54}$-$(Zr_{0.54}Ti_{0.46})O_3$ ceramics with temperature.

temperature of the undoped $Pb(Zr_{0.54}Ti_{0.46})O_3$ ceramic was reported as 385 °C [9]. La addition at 1 at% level caused a large decrease in the Curie temperature of this ceramic; the T_C was measured as 339 °C. The PSLZT ceramic with 1 at% La and 5 at% Sr had a T_C of 272 °C. Since Sr and La exhibit similar straining effects on the perovskite lattice the drop in T_C was consistent with studies reported in the literature [9,23]. The trend of lower T_C in the presence of Sr has been observed in other PZT families, the effect has been correlated with the ease of transformation from T phase to R modification at lower temperatures due to the smaller size of the dopants [36].

4. Conclusions

PZT ceramics modified with simultaneous additions of Sr and La were produced with pure perovskite structure through conventional ceramic processing techniques. The incorporation of Sr^{2+} into the PZT lattice stabilized the tetragonal symmetry over the rhombohedral one and enhanced the grain growth during sintering. Although La had similar effect on the stability of the tetragonal phase it had the tendency of decreasing the grain size. In the co-doped ceramics, satisfactory densification could be attained due to effective development of the microstructure consisting of a mixture of large and small grains.

Combination of Sr and La as co-dopants had great implications on the dielectric and piezoelectric properties of the PZT ceramics. A remarkably high strain coefficient d_{33} of 640 pC/N was attained in the PSLZT ceramic containing 1 at% La and 5 at% Sr, the Zr/Ti ratio being the one on the MPB. The Curie temperature of this particular ceramic was 272 °C.

Acknowledgement

The authors are grateful to the State Planning Organization (DPT) of Turkey for financial support of this research through Faculty Development Program (OYP) Project No.: 2002K120510.

References

[1] B. Jaffe, W.R. Cook, H. Jaffe, Piezoelectric Ceramics, Academic Press, London, 1971.
[2] S.S. Chiang, M. Nishioka, R.M. Fulrath, J.A. Pask, Effect of processing on microstructure and properties of PZT ceramics, Am. Ceram. Soc. Bull. 60 (1981) 484–489.
[3] L. Wu, C.C. Wei, T.S. Wu, H.C. Liu, Piezoelectric properties of modified PZT ceramics, J. Phys. C: Solid State Phys. 16 (1983) 2813–2821.
[4] Z. Weilie, Z. Peilin, L. Sidong, Piezoelectric ceramics with high coupling and high temperature stability, Ferroelectrics 101 (1990) 173–177.
[5] S.K. Nag, D.C. Agrawal, Piezoelectric and mechanical properties of ceria-doped lead zirconate titanate ceramics, J. Mater. Sci. 27 (1992) 4125–4130.
[6] C. Moure, M. Villegas, J.F. Fernandez, P. Duran, Microstructural and piezoelectric properties of fine grained PZT ceramics doped with donor and/or acceptor cations, Ferroelectrics 127 (1992) 113–118.
[7] T. Yamamoto, Optimum preparation methods for piezoelectric ceramics and their evaluation, Am. Ceram. Soc. Bull. 71 (1992) 978–985.
[8] J.F. Fernandez, C. Moure, M. Villegas, P. Duran, M. Kosec, G. Drazic, Compositional fluctuations and properties of fine-grained acceptor-doped PZT ceramics, J. Eur. Ceram. Soc. 18 (1998) 1695–1705.

[9] F. Kulcsar, Electromechanical properties of lead titanate zirconate ceramics with lead partially replaced by calcium or strontium, J. Am. Ceram. Soc. 42 (1959) 49–51.
[10] P.R. Chowdhury, S.B. Deshpande, Effect of dopants on the microstructure and lattice parameters of lead zirconate–titanate ceramics, J. Mater. Sci. 22 (1987) 2209–2215.
[11] C.K. Liang, L. Wu, Microstructure and properties of Cr_2O_3-doped ternary lead zirconate titanate ceramics, J. Am. Ceram. Soc. 76 (1993) 2023–2026.
[12] R. Lal, R. Krishnan, P. Ramakrishnan, Transition between tetragonal and rhombohedral phases of PZT ceramics prepared from spray-dried powders, Br. Ceram. Trans. J. 87 (1988) 99–102.
[13] S.W. Lin, C.P. Chin, T.K. Fan, K.C. Kao, Effects of electric and magnetic fields on the resonance frequency of piezoelectric ceramics, Ferroelectrics 88 (1988) 67–71.
[14] C.A. Randall, N. Kim, J.P. Kucera, W. Cao, T.R. Shrout, Intrinsic and extrinsic size effects in fine-grained morphotropic-phase boundary lead zirconate titanate ceramics, J. Am. Ceram. Soc. 81 (1998) 677–688.
[15] C. Bedoya, Ch. Muller, J.-L. Baudour, V. Madigou, M. Anne, M. Roubin:, Sr-doped $PbZr_{1-x}Ti_xO_3$ ceramic: structural study and field induced reorientation of ferroelectric domains, Mater. Sci. Eng. B75 (2000) 43–52.
[16] G.H. Haertling, C.E. Land, Hot-pressed $(Pb,La)(Zr,Ti)O_3$ ferroelectric ceramics for electrooptic applications, J. Am. Ceram. Soc. 54 (1971) 1–11.
[17] A. Garg, D.C. Agrawal, Effect of rare earth (Er, Gd, Eu, Nd and La) and bismuth additives on the mechanical and piezoelectric properties of lead zirconate titanate ceramics, Mater. Sci. Eng. B86 (2001) 134–143.
[18] D. Kuscer, J. Korzekwa, M. Kosec, R. Skulski, A- and B-compensated PLZT x/90/10: sintering and microstructural analysis, J. Eur. Ceram. Soc. 27 (2007) 4499–4507.
[19] C. Galassi, D. Piazza, F. Craciun, P. Verardi, Electrical investigation of sintering factors influence on PLZT ceramics, J. Eur. Ceram. Soc. 24 (2004) 1525–1528.
[20] A. Tawfik, Elastic properties of sound wave velocity of PZT transducers doped with Ta and La, J. Am. Ceram. Soc. 68 (1985) 317–319.
[21] M. Hammer, M.J. Hoffmann, Detailed X-ray diffraction analyses and correlation of microstructural and electromechanical properties of La-doped PZT ceramics, J. Electroceram. 2:2 (1998) 75–84.
[22] L. Pdungsap, N. Udomkan, S. Boonyuen, P. Winotai, Optimized conditions for fabrication of La-dopant PZT ceramics, Sens. Actuators A 122 (2005) 250–256.
[23] B. Praveenkumar, H.H. Kumar, D.K. Kharat, B.S. Murty, Investigation and characterization of La-doped PZT nanocrystalline ceramic prepared by mechanical activation route, Mater. Chem. Phys. 112 (2008) 31–34.
[24] F. Kulcsar, Electromechanical properties of lead titanate zirconate ceramics modified with certain three- or five-valent additions, J. Am. Ceram. Soc. 42 (1959) 343–349.
[25] P.K. Mehta, B.D. Padalia, M.V.R. Murty, A.M. Varaprasad, K. Uchino, X-ray structural determinations on Sr and La doped PZT, Ferroelect. Lett. 7 (1987) 121–129.
[26] K. Ramam, K. Chandramouli, Dielectric and piezoelectric properties of combinatory effect of A-site isovalent and B-site acceptor doped PLZT ceramics, Ceramics-Silikaty 53 (2009) 189–194.
[27] M.A. Mohiddon, K.L. Yadav, Effect of heating rate on dielectric and pyroelectric properties of double doped PZT, Adv. Appl. Ceram. 107 (2008) 310–317.
[28] T. Senda, R.C. Bradt, Grain growth in sintered ZnO and $ZnO–Bi_2O_3$ ceramics, J. Am. Ceram. Soc. 73 (1990) 106–114.
[29] R.A. Langman, R.B. Runk, S.R. Butler, Isothermal grain growth of pressure-sintered PLZT ceramics, J. Am. Ceram. Soc. 56 (1973) 486–488.
[30] X. Dai, A. DiGiovanni, D. Viehland, Dielectric properties of tetragonal lanthanum modified lead zirconate titanate ceramics, J. Appl. Phys. 74 (1993) 3399–3405.
[31] M.J. Hoffmann, M. Hammer, A. Endriss, D.C. Lupascu, Correlation between microstructure, strain behavior, and acoustic emission of soft PZT ceramics, Acta Mater. 49 (2001) 1301–1310.
[32] K Okazaki, K. Nagata, Effects of grain size and porosity on electrical and optical properties of PLZT ceramics, J. Am. Ceram. Soc. 56 (1973) 82–86.
[33] S.J. Yoon, A. Joshi, K. Uchino, Effect of additives on the electromechanical properties of $Pb(Zr,Ti)O_3–Pb(Y_{2/3}W_{1/3})O_3$ ceramics, J. Am. Ceram. Soc. 80 (1997) 1035–1039.
[34] C.H. Wang, The piezoelectric and dielectric properties of PZT-PMN-PZN, Ceram. Int. 30 (2004) 605–611.
[35] R.S. Nasar, M. Cerqueira, E. Longo, J.A. Varela, A. Beltran, Experimental and theoretical study of the ferroelectric and piezoelectric behavior of strontium-doped PZT, J. Eur. Ceram. Soc. 22 (2002) 209–218.
[36] H. Zheng, I.M. Reaney, W.E. Lee, N. Jones, H. Thomas, Effects of Sr substitution in Nb-doped PZT ceramics, J. Eur. Ceram. Soc. 21 (2001) 1371–1375.